Covalent functionalization of polycrystalline silicon nanoribbons applied to Pb(II) electrical detection

Brice Le Borgne, Aurelie Girard, Christophe Cardinaud, Anne-Claire Salaün, Laurent Pichon, Florence Geneste

Covalent functionalization of polycrystalline silicon nanoribbons applied to Pb(II) electrical detection

Brice Le Borgne[a,+], Aurélie Girard[b], Christophe Cardinaud[b], Anne-Claire Salaün[a], Laurent Pichon[a,+] and Florence Geneste[c,+]

[a]Institut d'Electronique et de Télécommunications de Rennes, équipe Microélectronique et Microcapteurs, UMR CNRS 6164, Université de Rennes 1, Rennes, France

[b]Institut des Matériaux de Nantes Jean Rouxel, Université de Nantes, Nantes, France

[c]Institut des Sciences Chimiques de Rennes, équipe MaCSE, UMR CNRS 6226, Université de Rennes 1, Rennes, France

[+]Corresponding authors: b.h.leborgne@surrey.ac.uk, florence.geneste@univ-rennes1.fr, laurent.pichon@univ-rennes1.fr

GRAPHICAL ABSTRACT

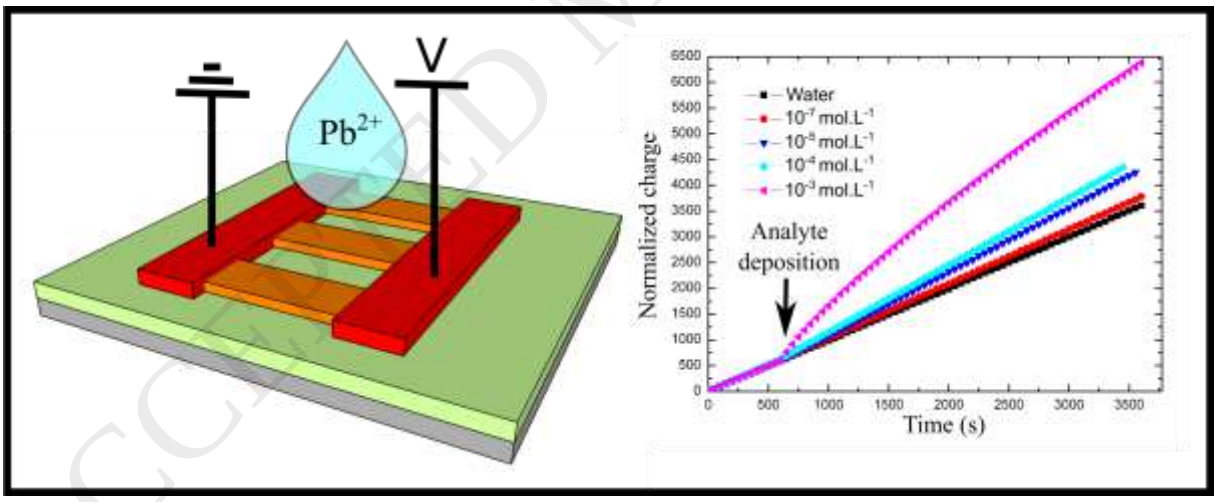

Abstract

Although recent studies in the field of nanomaterials have allowed the realization of highly sensitive sensors, research regarding new types of functionalization of nanostructures to reach high selectivity are still missing. Here, a simple electronic device based on polycrystalline

silicon (poly-Si) nanoribbons used for lead detection is presented. This device is functionalized by reduction of aryl diazonium salts in order to detect heavy metals. The effectiveness of the grafting process and thickness homogeneity of the coating layer were evaluated by XPS and NanoSIMS techniques. The preconcentration of lead (Pb^{2+}) at the surface of the functionalized nanostructures was substantially verified. Finally, electrical characterization of the resistors based on the functionalized nanoribbons, showed that the sensitivity to these species is increased in the concentration ranging from 10^{-7} to 10^{-5} mol L^{-1}. This technique could pave the way for use of complexing agents to enhance heavy metal detection.

Keywords: Silicon nanoribbons; Aryl-diazonium salts; Functionalization;

Chemical sensors.

1. Introduction

Lead is one of the heavy metals, of which its presence in water at high concentrations has become a growing concern. Heavy metals form an important class of pollutants [1]. They can be found in water naturally but also due to mining, agriculture and industry. Detecting and eliminating heavy metals is of concern because they are highly persistent and not generally degraded by bacteria. They are toxic and their accumulation in living cells leads to serious pathologies [2]. Some heavy metals have been subject to severe regulations due to high levels of toxicity even in trace amounts. Thus, exposure to heavy metals may result in cancer, damage to the kidneys and even death in some cases where concentration levels are very high [3].

The mass production of silicon based components allows the realization of low-cost, easy to process and fully embeddable electronic raw material. Polycrystalline silicon (poly-Si) is one of the many forms of silicon, which is composed of a combination of silicon crystals and

grain boundaries that are formed during crystallization process. Poly-Si is prepared by layer deposition and is used in a variety of applications, such as thin film transistors (TFTs) [4,5], solar cells [6,7], strain gauges [8,9] or diodes [10]. One of its deposition technique is Low-Pressure Chemical Vapor Deposition (LPCVD) which can provide good homogeneity of the silicon in terms of thickness, doping concentration and stability.

Most electronic sensors are based on field effect transistors (FETs) which have proven high sensitivity and electrical performances [11-13]. However, they require several photolithography processes, plasma etching and deposition steps that can provide reproducibility drawbacks. In contrast, new passive devices such as resistors have recently shown that they enable chemical species detection, exhibiting low detection limits (e.g. for gases [14] or biological materials [15]). More specifically, poly-Si is very sensitive to charged species although its fabrication process is less demanding and cheaper.

Nanostructures such as nanowires [16-18] or nanoribbons [19,20] can be obtained from few nanometers thick poly-Si layers by LPCVD at low temperature (< 600°C) [21,22]. These nanostructures offer interesting potential for chemical species detection so far as their high surface/volume ratio enables them to have a high exchange surface between analyte and sensitive material. Furthermore, they can be easily functionalized using miscellaneous materials such as antibodies [23] or DNA [24] in order to reach selectivity to targeted species. Aryl-diazonium salts are frequently used to functionalize semiconductors [25], particularly crystallized silicon-based surfaces [26] and their spontaneous grafting on poly-Si layers has been previously demonstrated [27]. This efficient and fast grafting process leads to a strong covalent bond and monolayers or thin films, can be obtained in well-controlled conditions [28,29]. Nevertheless, the potential of aryl diazonium grafting at the nanostructures surface has been marginally investigated to date [30,31].

The interest of a complexing agent to accumulate heavy metal ions at the surface of sensors has been previously demonstrated. Indeed, some complexing agents for Cd [32], Pd [33] and Pb [32] ions have been already immobilized on surfaces by reduction of their diazonium salts. The use of complexing agents to accumulate ions (i.e. in aqueous solution) at the surface of a resistor based on poly-Si nanostructures has not been investigated and requires exploration. The coating layer would be expected to give a higher sensitivity to the sensors.

In this work, we present a simple resistor based on poly-Si nanoribbons for heavy metal detection. The presented device is formed by a row of nanoribbons which is fully compatible with CMOS technology and enables direct *in-situ* measurement. These nanoribbons were functionalized with aryl diazonium salts containing complexing groups in view of using this type of structure for heavy metal detection. The effectiveness of the grafting process is evaluated. After which, the preconcentration of lead ions (Pb^{2+}), chosen as an example of heavy metal ion, at the surface of the functionalized nanostructures is checked. Finally, an electrical characterization of the sensor shows that the coating layer increases the detection capabilities.

2. Materials and methods

2.1 Devices fabrication

Silicon nanostructures were formed on a cleaned silicon wafer and native oxide was removed by chemical etching using a diluted HF solution (2%). A 1.2 µm thick SiO_2 insulating layer was deposited by Atmospheric Pressure Chemical Vapor Deposition (APCVD) technique at 420°C using silane (SiH_4) and dioxygen (O_2) gas sources. Amorphous silicon was deposited by LPCVD at 550°C at 90 Pa using SiH_4 source and crystallized during an annealing step at 600°C for 12 hours in order to obtain a 50 nm thick poly-Si layer. The layer underwent photolithography and was etched using SF_6 plasma reactive ion etching (RIE). Thus, 500 parallel nanoribbons (Fig. 1a) were formed. The length (L) and width (W) of these

nanoribbons were 8 µm and 5 µm, respectively. A protective 100 nm thick SiO_2 layer was deposited following APCVD. SiO_2 was etched in order to open a window on each side of the nanoribbons (Fig. 1b). This layer enabled the deposition of heavily *in-situ* doped N-type poly-Si layer using SiH_4 and phosphine (PH_3) sources for the formation of contact electrodes. This last layer was etched by SF_6 plasma RIE. Finally, the protective layer was etched using HF (2%) (Fig. 1c). Fig. 1d presents a SEM image of the obtained device.

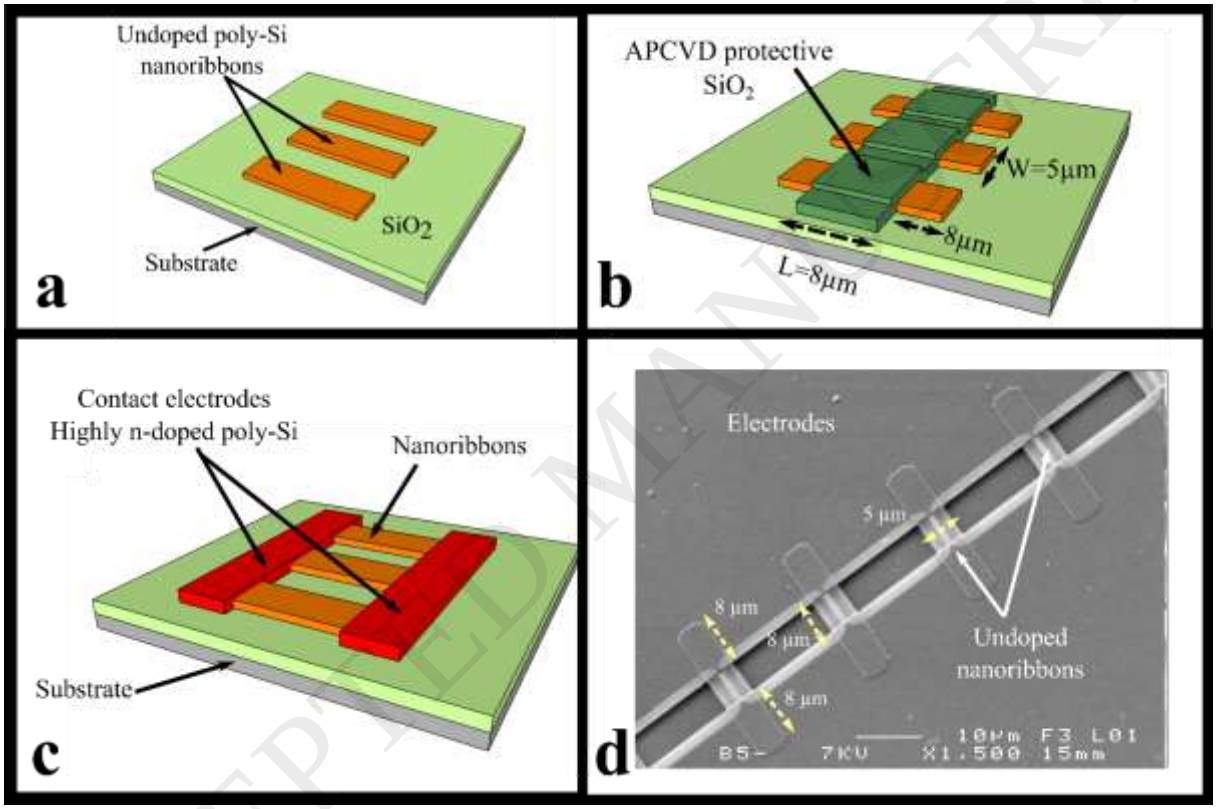

Fig. 1 3-dimensional sketches of the fabrication process. (a) Deposition and formation of 500 parallel undoped poly-Si nanoribbons (50 nm thick) on an APCVD deposited SiO_2 layer. (b) Deposition and formation of an SiO_2 protective layer. (c) Deposition and formation of the highly doped poly-Si contact electrodes and removal of the protective layer. (d) SEM top view of the device with geometric parameters: L=8µm and W=5 µm.

2.2 Chemical

The resistor was functionalized by spontaneous grafting of aryl diazonium salts (Fig. 2) according to the following protocol, described in previous studies [34]. All manipulations were carried out under argon using a Schlenk line with standard airless techniques. A 2% hydrofluoric acid solution was cannulated into a reactor cell, which contained the samples under argon, in order to remove the native Si oxide. After 15 seconds of immersion, the HF solution was eliminated. A solution of 4-carboxymethyl-benzenediazonium salts or 4-iodo-benzenediazonium salts was prepared by addition of 0.25 mL of isopentyl nitrite to 17 mg of 2-(4-aminophenyl)acetic acid or 20 mg of 4-iodoaniline dissolved in 120 mL of deoxygenated acetonitrile (HPLC grade) at 0°C for 15 minutes. This solution was then cannulated into the reactor cell. The samples were kept in the solution at 0°C for 15, 30, 60 or 180 minutes. The devices were then washed in three successive baths of acetonitrile of 5 minutes each. The solutions of lead for electrical tests were prepared from $Pb(NO_3)_2$ in ultrapure water.

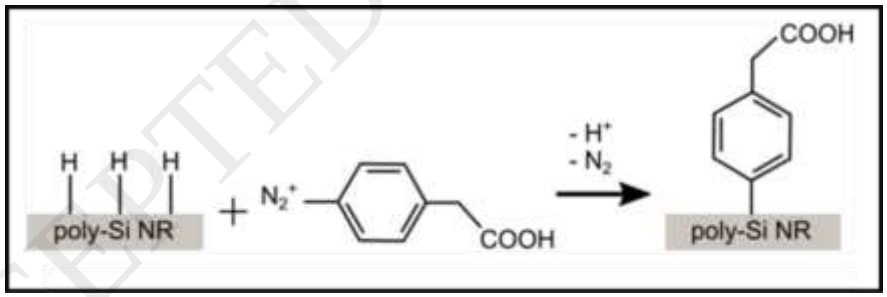

Fig. 2 Spontaneous grafting of carboxylate-terminated aryl diazonium salts at the surface of polycrystalline silicon nanoribbons.

2.3 Instrumentation

Layers thicknesses were obtained using HORIBA Uvisel 2 Ellipsometer. The swept spectral range was from 200 nm to 2100 nm and with the incident angle on the sample fixed at 70°. The following values were taken for poly-Si base layer: n = 3.85, k = 0.016 at 632 nm. The

optical constants of the layer were determined using the classical Lorentz oscillator dispersion formula. The values were measured on clean surfaces before grafting and the layers thicknesses were determined from the same plates after modification, taking n = 1.65, k = 0 for the layer. Measurements reported are the average of five data points across the substrate.

X-ray photoelectron spectroscopy (XPS) has been carried out with a Kratos Axis Nova HSA spectrometer using a monochromatic Al Kα excitation (1486.6 eV), with magnetic confinement charge neutralization. The lens low magnification mode was used with the slot aperture resulting in an analysed area of 700 per 300 μm^2. Charge stabilization was achieved by using the Kratos Axis internal device. Survey scans were recorded with an energy step of 0.5 eV and a pass energy (PE) of 80 eV. High resolution spectra were acquired at 20 eV PE and a step of 0.1 eV. In these conditions, the energy resolution gives a full width at half maximum (FWHM) of the $Ag3d_{5/2}$ peak of about 0.55 ± 0.02 eV. The photoelectron take-off angle was 90° with respect to the sample plane, which provides an integrated sampling depth of approximately 15 nm. Chemical images were recorded at 80 eV PE using the small spot aperture and high-resolution iris settings leading to 400 per 400 μm^2 images with a pixel resolution of ~2 µm. Data analysis was done with the CasaXPS software [35].
It is worth noting that the grafted layer was still observed in XPS when the samples were sonicated 3 times in acetonitrile for 5 minutes.

NanoSIMS analyses were performed on a NanoSIMS 50 standard ion microprobe (Cameca). The samples were cut and directly introduced into the chamber. An oxygen primary ionic source was used for the measurement of ^{208}Pb. A 17 keV O-beam (~30 pA) was focused and raster-scanned on the surface sample. Sputtered positive secondary ions were extracted for mass analysis and collected in an electron multiplier. A mass resolving power of ~5500 ($M/\Delta M$) was enabled to remove potential mass interferences. All ^{208}Pb images (50µm

×50µm) of the same set were recorded under the same primary ion current and with the same parameters (diaphragms, slits, time/pixel). The spatial resolution for all images was 400 nm.

3. Results and discussion

3.1 Ellipsometry

The working principle of the sensor is based on the ions charges influence on the semiconductor (poly-Si). Consequently, it is crucial to ensure that the coating film thickness does not exceed a few nanometers, as it would lead to charge screening, which would prevent charge detection. Thus, the thickness of the coating film was measured by ellipsometry. This was performed on a 50 nm thick poly-Si layer. Fig. 3 shows that thickness increases with the grafting time. During the first hour of grafting, the deposition rate was about 6 nm/hour whereas during the two following hours, this rate decreased to about 0.5 nm/hour, showing a saturation of the thickness. These observations are in accordance with existing literature [36].

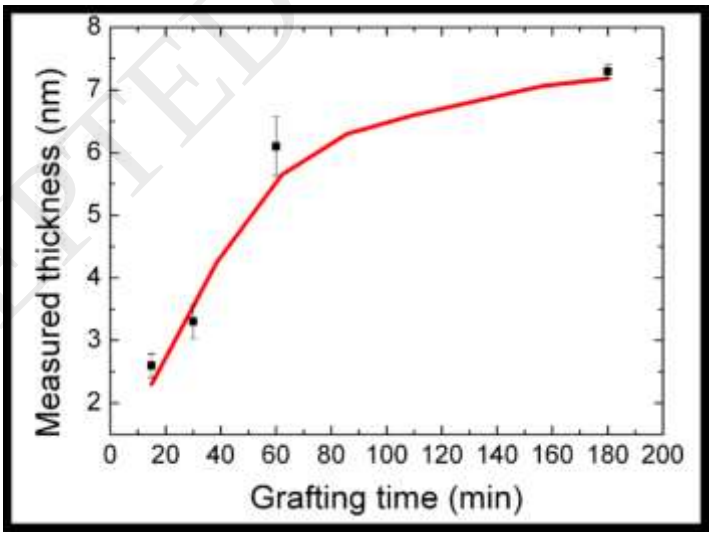

Fig. 3 Film thicknesses measured by ellipsometry as a function of grafting time. Each thickness was measured 5 times at different locations. Error bars correspond to the maximum and minimum thicknesses measured for the 5 locations.

3.2 XPS analyses

XPS analysis was performed to ensure that the grafting of diazonium salts was effective. In this view 4-iodo-benzenediazonium salts were used in which, iodine was used as a specific chemical XPS marker. The protocol for the grafting process was similar to those of the carboxylate layer. 50 nm thick polycrystalline silicon layers were prepared and grafted (see experimental section) with an immersion time of 30 minutes (thickness ≈ 3.5 nm) and 1 hour (thickness ≈ 6 nm). Analysis were done on a non-grafted poly-Si layer and different parts of processed devices. Fig. 4a presents grafting results on poly-Si part of the grafted device for 30min and 1 hour, compared to a poly-Si non-grafted sample. For the device, sample analysis was carried out at the centre of a nanoribbon connection pad (800 × 800 µm). As shown on the figure, no iodine is detected on the non-grafted poly-Si, whereas a significant I 3d signal is observed for the grafted surfaces. Moreover, the signal intensity follows the grafting time. Fig. 4b compares iodine I 3d signal for the 30 minutes grafted device on the poly-Si pad and the SiO_2 base layer. It seems that the grafting process preferentially takes place on the poly-Si, whereas an organic layer was probably also formed on the SiO_2 area. Indeed, after treatment with diluted HF, the SiO_2 surface give some Si-H bonds that are known to spontaneously react with diazonium salts [21].

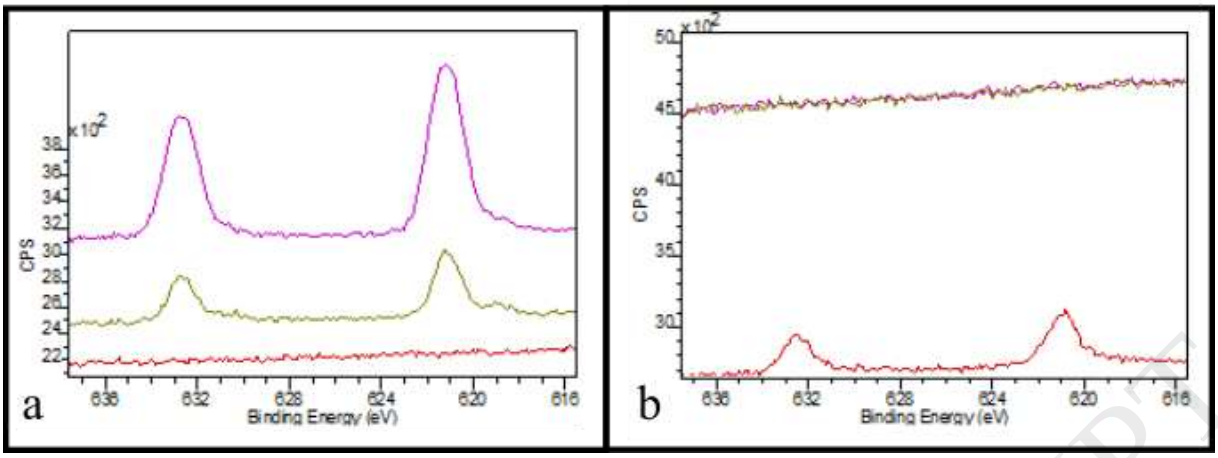

Fig. 4 Grafting efficiency verification. (a) XPS iodine I 3d spectral region (range 616 eV to 638 eV) of a 50 nm thick poly-Si non-grafted layer (red), after 30 minutes (green) and 1 hour (pink) of grafting with iodine-terminated salts on poly-Si pad. (b) XPS iodine I 3d spectral region on SiO_2 (green - 30 min, pink - 1 hour) and poly-Si (red - 30 min) parts of the grafted device.

To confirm the efficiency of the grafting process at the micrometric level, XPS images were performed on the same device. Analysis was carried out on a poly-Si cross pattern of 30 µm width and comb-like structures on SiO_2 whose width was 5 µm, corresponding to the width of the nanoribbons (see Fig. 5a). Indeed, the nanoribbons have not been directly imaged because they remain difficult to spot, using this technique. However, it has been achieved on structures of comparable dimensions. XPS imaging of a surface consisted of choosing a binding energy representing a core level from the element of interest (here, poly-Si (Si 2p at 99.3 eV), SiO_2 (Si 2p at 103.3 eV) and iodine (I $3d_{5/2}$ at 621.2 eV)), acquiring an image then taking a second image at an energy representative of the background signal for the photoelectron peak previously measured. Once the peak and background images are done, interpretation of the results was based on the difference in counts per second between the peak and the background images. The XPS images obtained from the analysis of silicon, silicon oxide and iodine

compounds after grafting are given in Fig. 5b, 5c and 5d, respectively. On the part of the pattern with poly-Si, the signal intensity related to the iodine compound is significantly higher than on the silicon oxide probably because of the higher effectiveness of the grafting process on poly-Si. Fig. 5d shows that the presence of iodine on the comb structures of 5 µm width and on the cross, is noted. The intensity of the signal is strong and relatively homogeneous along these structures. This confirms the efficiency of the grafting and its homogeneity along nanostructures of poly-Si of 50 nm thickness.

These analyses show that a simple dip coating process in a solution of diazonium salts allows the homogeneous functionalization of nanostructures composed of polycrystalline silicon thin films (50 nm thick). Note that to our knowledge, this is the first study reporting the covalent grafting of aryl-diazonium salts on non-intentionally-doped thin silicon layers. Further experiments were then carried out to check the efficiency of the carboxylate-modified layer deposited on the nanoribbons to complex lead ions.

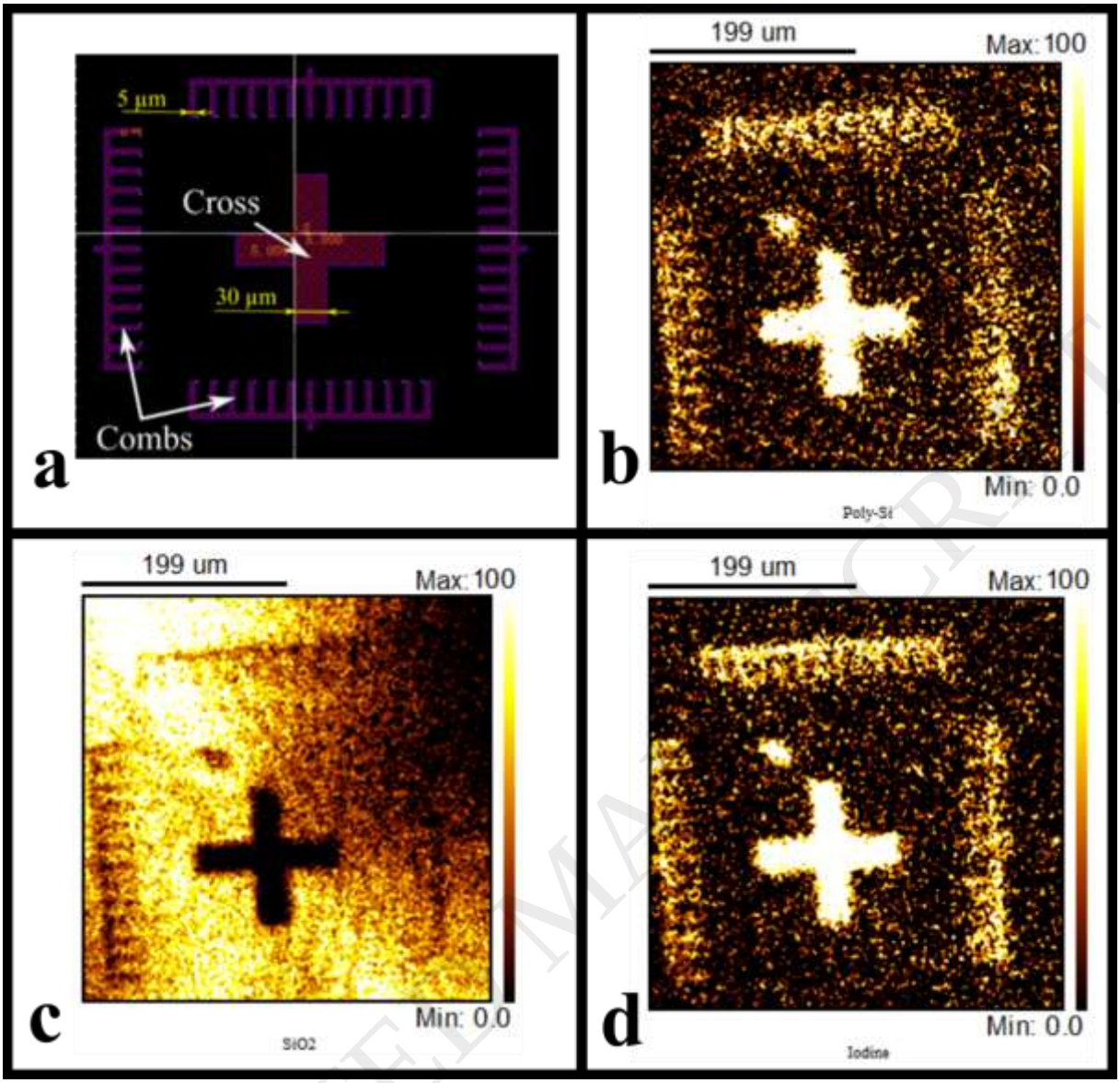

Fig. 5 XPS imaging of the cross pattern based device. (a) Cross and combs shapes used for XPS imaging of salts grafting. Combs geometry (width equals 5 µm) are the same as the sensors nanoribbons. (b) Grafted sample, image acquired at 99.3 eV (BE) corresponding to the maximum of the Si 2p (Si). (c) Grafted sample, image acquired at 103.3 eV corresponding to the maximum of the Si 2p (SiO_2). (d) Grafted sample, image acquired at the I $3d_{5/2}$ binding energy (621.2 eV).

3.3 NanoSIMS analysis

A comparison of non-grafted and grafted structures was performed by the analysis of the isotope 12 of carbon (^{12}C) by NanoSIMS imagery. The results are presented in Fig. 6; these measurements have been performed simultaneously. Consequently, the samples have been exposed to the same level of ion beam, which means that the intensities were comparable. Before the grafting process (Fig 6a), the signal intensity was low, showing that the sample contained a very small amount of carbon on its surface. After functionalization (Fig 6b), the signal intensity drastically increased. Interestingly, a red colour was observed on all the samples, including i) nanoribbons, ii) contact electrodes and iii) SiO_2 zones between each nanoribbon. Owning to the high sensitivity of this imaging technique, no difference in the effectiveness of the grafting process according to the nature of the surface (poly-Si or SiO_2) was observed. These results underline the effectiveness of the grafting process to modify the poly-Si nanostructures, confirming XPS analyses.

To ensure that immobilized carboxylate groups are able to trap lead ions, unmodified and modified samples were exposed to a Pb^{2+} solution (10^{-3} mol L^{-1}) for 15 minutes, corresponding to a thickness of 2.5 nm. The samples were then rinsed by immersion in isopropanol and dried. The analysis of the device was done targeting isotope 128 of lead (^{128}Pb). For the non-grafted device (Fig. 6c), the signal was low, highlighting that the amount of lead on its surface was negligible. Conversely, the signal intensity was high on the grafted structure (Fig. 6d). These results underline the role of the carboxylate groups to preconcentrate lead ions on the surface by complexation, as it has been observed previously [37].

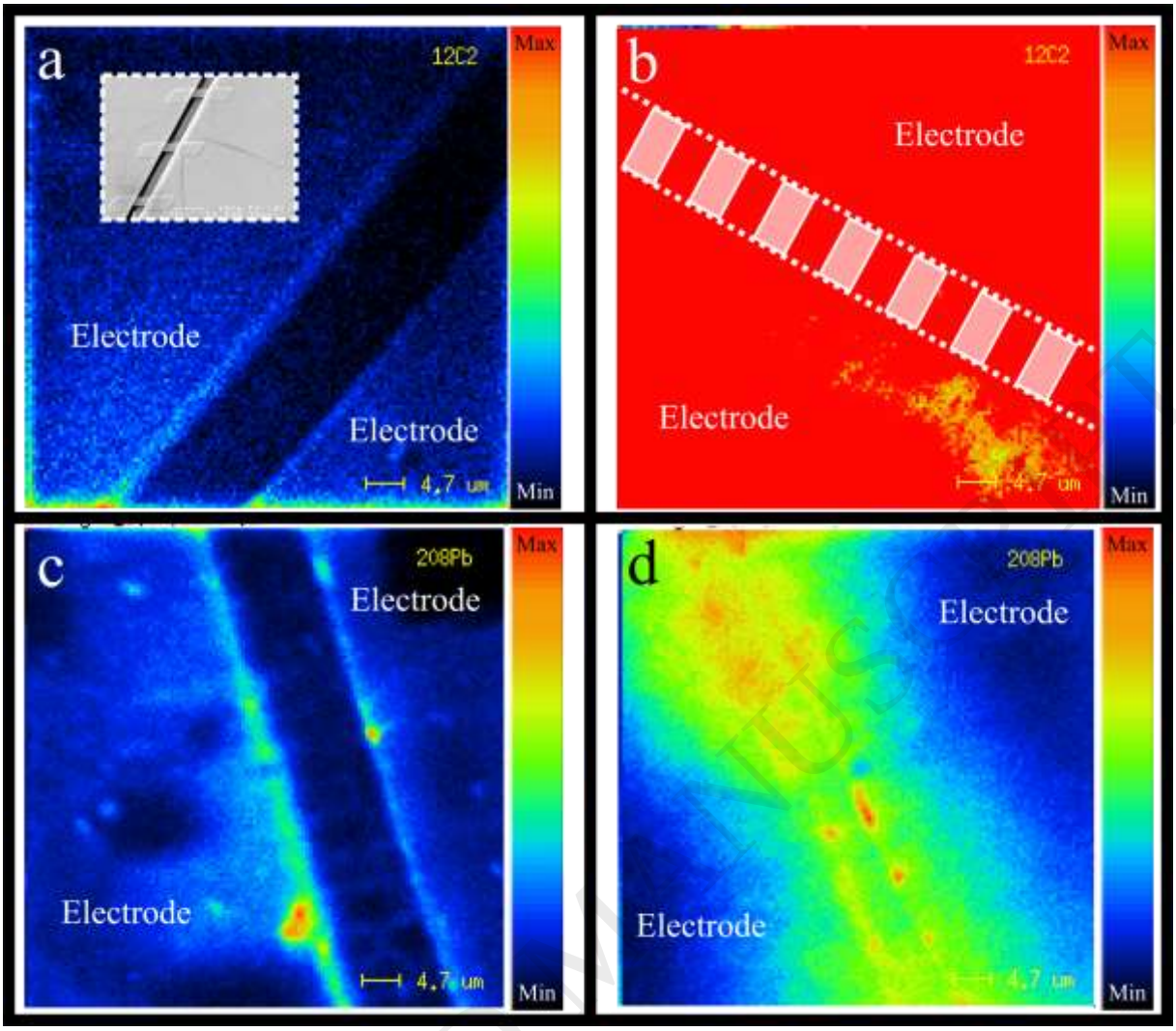

Fig. 6. NanoSIMS imaging of the nanoribbons-based device. ^{12}C element tracking before (a) and after (b) grafting process. Inset is a corresponding SEM view of the device. ^{208}Pb tracking after 15 minutes exposure to lead solution before (c) and after (d) grafting process.

3.4 Electrical characterization

Electrical analysis of the nanoribbons-based resistors has been performed in order to highlight any interesting grafting effects on the lead detection. It is worth noting that during the set of experiments, the coating layer has been chosen as thin as possible to avoid any charge screening effect, due to the insulating nature of diazonium salts [29]. Consequently, the

grafting step was performed during 15 minutes (thickness ≈ 2.5 nm). The analysis is based on the measurement of the charge quantity flowing through the resistor (biased at 1V) and calculated in real-time by integrating current as a function of time: $q(t) = \int_0^t i(\tau)d\tau$, where q is the charge and i is the current. Indeed, the influence of ions on silicon is related to the supply of surface charges and therefore, it has been considered as interesting and should be evaluated.

For an easier comparison of the performances of the different devices, the measured charges were normalized by the first charge value Q_0 measured at t_0 = 1 s from the initial current I_0. Since the measurement time step Δt was set to 1 s, the value of the normalized load is thus obtained by making a discrete sum as follows:

$$\frac{q(t)}{Q_0} = \frac{\sum_{t0}^{t} i(\tau)\times d\tau}{I_0 \times t_0} \quad (1)$$

Firstly, normalized charge was recorded as a function of time after exposure of the modified nanoribbons to different concentrations of analytes. As shown in Fig. 7, the functionalized devices were exposed to deionized water and to different concentrations of lead solutions, ranging from 10^{-7} to 10^{-3} mol L^{-1}. These solutions were prepared following the protocol detailed in the experimental section. Before the analyte deposition, the normalized charge of all devices increased linearly in the same way whereas the current remains constant. After the deposition, the higher the concentration of Pb^{2+} was, the more the normalized charge increased. For the sample exposed to water, no slope change was noted. These results show that the detection of ions is effective and depends on solution concentration. Moreover, the detection of ions is effective and depends on the solution concentration. It also highlights that such a sensor could be used for real-time on-site measurements, its response showing sufficient slope changes depending on the concentration after 10 minutes exposure time.

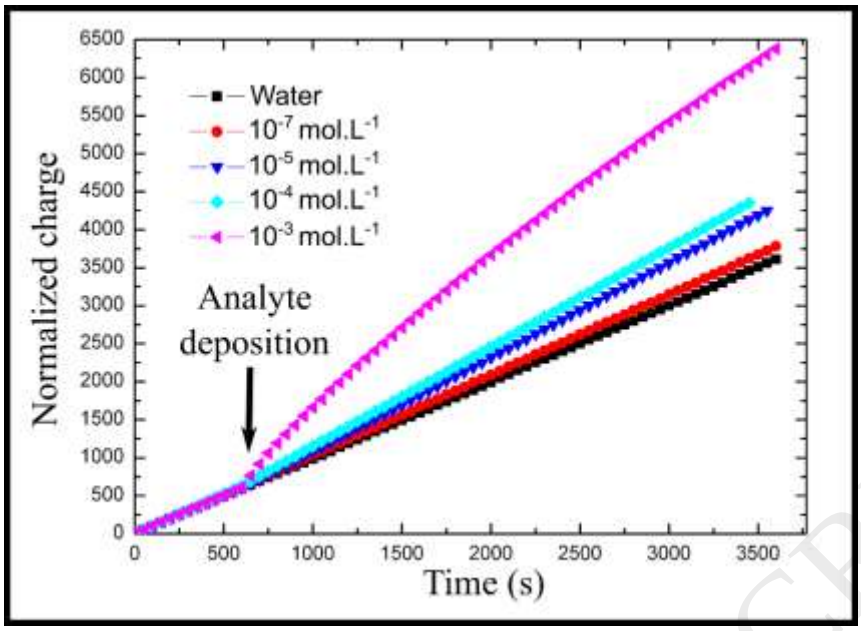

Fig. 7 Normalized charge measurement as a function of time on modified poly-Si nanoribbons (50 nm thick) based resistors. Samples were exposed to deionized water and to lead solution, of which concentrations were 10^{-7}, 10^{-5}, 10^{-4} and 10^{-3} mol L^{-1}.

Fig. 8 presents the measurements obtained for different concentrations of lead solutions. Fig. 8a illustrates the normalized charge obtained for different Pb^{2+} concentrations after 1, 2, 5, 10 and 50 minutes exposure of the sensor to these solutions. The volume of solution used for these experiments was lower than 1 mL. Error bars represent the dispersion of values for 5 different devices, tested one by one, at room temperature. The insulation of the contact electrodes was checked (Fig. S1). For periods of less than 10 minutes exposure, no clear increase of the charge was observed (Fig. 8a). The normalized charge significantly increased with concentration when the time of exposure to the ions was greater than 10 minutes, showing an influence of the Pb^{2+} charges on the poly-Si.

We consequently studied the sensor response for an exposure time ranging from 10 to 50 minutes and checked the influence of the carboxylate layer on the measured charge. The

characterization of the devices, with and without functionalization of the nanoribbons, was performed to ascertain if the preconcentration of lead ions on the surface significantly impacts the quality of the detection. The normalized charge for 10, 30 and 50 minutes for concentrations ranging from 10^{-8} to 10^{-4} mol L^{-1} is presented in Fig. 8b, 8c and 8d, respectively.

The red curve, corresponding to the non-grafted structures, does not seem to show any real trend. The charge decreases when the concentration increases to the middle of the measured range (around 10^{-6} mol L^{-1}) and then increases with the concentration up to 10^{-4} mol L^{-1}. For the grafted structures (black curve), the quantity of charges increases with the concentration. This phenomenon can be explained by the presence of Pb^{2+} charges, preconcentrated at the surface by complexation with the carboxylate groups, which influence the conduction in the semiconductor. The resistivity of the overall material (poly-Si/salts/Pb^{2+}) decreases and the calculated charge increases. When the grafted and non-grafted structures are compared, three zones corresponding to different electrical behaviours can be distinguished. These zones are denoted as A, B and C.

In zone A, ranging from 10^{-8} to 2×10^{-7} mol L^{-1}, there is no noticeable difference between the response of the sensor in the grafted and non-grafted configurations, probably because the sensor is not sensitive enough to detect Pb^{2+} ions at concentrations lower than 2×10^{-7} mol L^{-1}. The error bars confirm that there is no clear trend. We observe the same uncertainty in zone C, ranging from 7×10^{-6} to 10^{-4} mol L^{-1}, where the dispersion of the measured data points becomes substantial, especially with the poly-Si device. This is probably due to the high concentration of the analysed solutions, leading to saturation of the carboxylate groups by lead ions and important unselective adsorption of ions on the surface. In contrast, in zone B (from to 2×10^{-7} to 7×10^{-6} mol L^{-1}) a significant difference is obtained, highlighting a higher

amount of charges for the coated device. Such an observation seems to show that in this concentration range, the preconcentration of the lead ions (II) on the surface of the functionalized poly-Si nanoribbons affects the charge of the device. A longer exposure time clearly enhances the difference between the charges obtained on unmodified and modified devices, as shown after 30 and 50 minutes of exposure to lead solutions (Fig. 8c and 8d). This behaviour, showing that modification of the surface is necessary and exacerbates detection in a well-defined range of concentrations has been frequently reported in literature with sensors based on a preconcentration of ions on their surface [38]. Note that no interference studies were performed in this work. However, one can assume that using molecules with termination such as 1,4,8-tri(carbamoylmethyl) hydroiodide (TETRAM), such a sensor could show selectivity to lead. Indeed, this compound has already proven selectivity to Pb^{2+} trapping [39]. Thus, the coating layer could be tuned to reach selective detection of a specific targeted species.

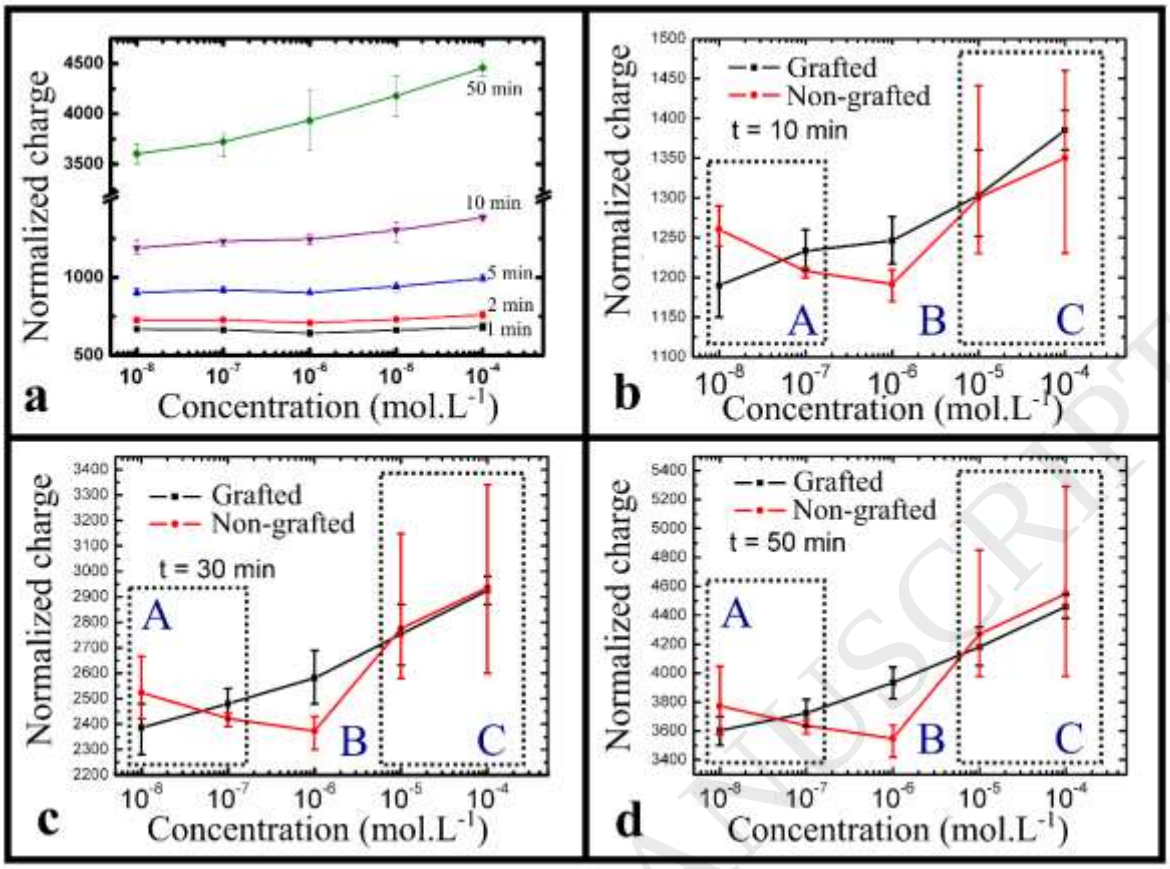

Fig. 8 Normalized charge measurement for different Pb^{2+} concentrations (a) and exposure times (1,2 5,10 and 50 min). Normalized charge comparison between grafted and non-grafted poly-Si nanoribbons based devices after 10 min (b), 30 min (c) and 50 min (d) exposure.

4. Conclusion

In this proof of concept study, a lead sensor based on polycrystalline silicon nanoribbons fabricated in a fully compatible CMOS silicon technology is demonstrated. The small volume of solution required for the analysis and the low dimensions of the device, combined with the benefits of nanoscale and microtechnology, make these devices promising as embeddable sensors in an autonomous system to monitor contamination on site.

Nanoribbons used as sensitive units are functionalized with an organic layer deposited by spontaneous grafting of diazonium salts. While this reaction is well-known on silicon, there are few studies on the grafting of diazonium salts on polycrystalline silicon nano-objects. The efficiency of the functionalization of these structures is underlined due to surface characterization techniques (ellipsometry, XPS and NanoSIMS). The functionalization made possible the preconcentration of ions contained in the analyte at the surface of the sensitive elements of the device.

Lead detection was checked by electrical measurements due to the influence of the lead on the electrical conductivity of Si-poly nanoribbons. Functionalization improves the accuracy of the sensor and increased its sensitivity. The lowest concentration where a noticeable difference exists between non-grafted and grafted devices (zone B) is 10^{-7} mol L^{-1}, which is very encouraging for this type of device, far from having reached maturity.

5. References

[1] H. Yongming, D. Peixuan, C. Junji, E.S. Posmentier, Multivariate analysis of heavy metal contamination in urban dusts of Xi'an, Central China. Sci. Total Environ. 355 (2006) 176-186.

[2] D.T. Dexter, F.R. Wells, A.J. Lee, F. Agid, Y. Agid, P. Jenner, C.D. Marsden, Increased nigral iron content and alterations in other metal ions occurring in brain in Parkinson's disease. J. Neurochem. 52 (1989) 1830-1836.

[3] R.C Patra, D. Swarup, S.K. Dwivedi, Antioxidant effects of α tocopherol, ascorbic acid and L-methionine on lead induced oxidative stress to the liver, kidney and brain in rats. Toxicology. 162 (2001) 81-88.

[4] R.E. Proano, R.S. Misage, D.G. Ast, Development and electrical properties of undoped polycrystalline silicon thin-film transistors. IEEE T. Electron. Dev. 36.9 (1989) 1915-1922.

[5] R. A. Sporea, M. Trainor, N. Young, J.M. Shannon, S.R.P. Silva, Temperature effects in complementary inverters made with polysilicon source-gated transistors. IEEE T. Electron. Dev., 62 (2015) 1498-1503.

[6] J. Dore, D. Ong, S. Varlamov, R. Egan, M.A. Green, Progress in laser-crystallized thin-film polycrystalline silicon solar cells: intermediate layers, light trapping, and metallization. IEEE J. Photovolt. 4 (2014) 33-39.

[7] C. Becker, D. Amkreutz, T. Sontheimer, V. Preidel, D. Lockau, J. Haschke, L. Jogschies, C. Klimm, J.J. Merkel, P. Plocic, B.Rech, Polycrystalline silicon thin-film solar cells: Status and perspectives. Sol. Ener. Mat. Sol. C. 119 (2013) 112-123.

[8] P.J. French, A.G.R. Evans, Piezoresistance in polysilicon and its applications to strain gauges. Solid state Electron. 32 (1989) 1-10.

[9] V. Mosser, J. Suski, J. Goss, E. Obermeier, Piezoresistive pressure sensors based on polycrystalline silicon. Sensor. Actuat. A-Phys. 28 (1991) 113-132.

[10] H.C. Card, E.H. Rhoderick, Studies of tunnel MOS diodes I. Interface effects in silicon Schottky diodes. J. Phys. D Appl. Phys. 4 (1971) 1589.

[11] P. Estrela, P. Migliorato, Chemical and biological sensors using polycrystalline silicon TFTs. J. Mater. Chem. 17 (2007) 219-224.

[12] O. Knopfmacher, M.L. Hammock, A.L. Appleton, G. Schwartz, J. Mei, T. Lei, J. Pei, Z. Bao, Highly stable organic polymer field-effect transistor sensor for selective detection in the marine environment. Nat. Commun. 5 (2014) 2954.

[13] S. Chen, A. van den Berg, E.T. Carlen, Sensitivity and detection limit analysis of silicon nanowire bio (chemical) sensors. Sensor. Actuat. B-Chem., 209 (2015) 486-489.

[14] K.M. Frazier, K.A. Mirica, J.J Walish, T.M. Swager, Fully-drawn carbon-based chemical sensors on organic and inorganic surfaces. Lab Chip 14 (2014) 4059-4066.

[15] M.G. Nikolaides, S. Rauschenbach, S. Luber, K. Buchholz, M. Tornow, G. Abstreiter, A.R. Bausch, Silicon- on- Insulator Based Thin- Film Resistor for Chemical and Biological Sensor Applications. ChemPhysChem 4 (2003) 1104-1106.

[16] A.C. Irvine, Z.A. Durrani, H. Ahmed, S. Biesemans, Single-electron effects in heavily doped polycrystalline silicon nanowires. Appl. Phys. Lett. 73 (1998) 1113-1115.

[17] L.C. Yen, T.M. Pan, C.H. Lee, T.S. Chao, Label-free and real-time detection of ferritin using a horn-like polycrystalline-silicon nanowire field-effect transistor biosensor. Sensor. Actuat. B- Chem. 230 (2016) 398-404.

[18] M.M.A Hakim, M. Lombardini, K. Sun, F. Giustiniano, P.L. Roach, D.E. Davies, P.H. Howarth, M.R.R. de Planque, H. Morgan, P. Ashburn, Thin film polycrystalline silicon nanowire biosensors. Nano Lett. 12 (2012) 1868-1872.

[19] I. Zeimpekis, K. Sun, C. Hu, N.M.J. Ditshego, O. Thomas, M.R.R. de Planque, H.M.H. Chong, H. Morgan, P. Ashburn, Dual-gate polysilicon nanoribbon biosensors enable high sensitivity detection of proteins. Nanotechnology 27 (2016) 165502.

[20] K. Sun, I. Zeimpekis, C. Hu, N.M.J. Ditshego, O. Thomas, M.R.R. de Planque, H.M.H. Chong, H. Morgan, P. Ashburn, Effect of subthreshold slope on the sensitivity of nanoribbon sensors. Nanotechnology, 27 (2016) 285501.

[21] L. Pichon, K. Mourgues, F. Raoult, T. Mohammed-Brahim, K. Kis-Sion, D. Briand, O. Bonnaud, Thin film transistors fabricated by in situ doped unhydrogenated polysilicon films obtained by solid phase crystallization. Semicond. Sci. Tech. 16 (2001) 918.

[22] T. Matsuyama, N. Terada, T. Baba, T. Sawada, S. Tsuge, K. Wakisaka, S. Tsuda, High-quality polycrystalline silicon thin film prepared by a solid phase crystallization method. J. Non-Cryst. Solids, 198 (1996) 940-944.

[23] E. Stern, J.F. Klemic, D.A. Routenberg, P.N. Wyrembak, D.B. Turner-Evans, A.D. Hamilton, D.A. LaVan, T.M. Fahmy, M.A. Reed, Label-free immunodetection with CMOS-compatible semiconducting nanowires. Nature, 445 (2007) 519.

[24] G. Godem-Wenga, E. Jacques, A.C. Salaün, R. Rogel, L. Pichon, F. Geneste, Polysilicon nanowires based field effect transistor compatible with MOS technology for integrated label-free direct detection of DNA hybridization. Biosensors (2012) 1.

[25] J. Pinson, F. Podvorica, Attachment of organic layers to conductive or semiconductive surfaces by reduction of diazonium salts. Chem. Soc. Rev. 34 (2005) 429-439.

[26] M. P. Stewart, F. Maya, D.V. Kosynkin, S.M. Dirk, J.J. Stapleton, C.L. McGuiness, D.L. Allara, J.M. Tour, Direct covalent grafting of conjugated molecules onto Si, GaAs, and Pd surfaces from aryldiazonium salts. J. Am. Chem. Soc. 126 (2004) 370-378.

[27] A. Girard, N. Coulon, C. Cardinaud, T. Mohammed-Brahim, F. Geneste, F. Effect of doping on the modification of polycrystalline silicon by spontaneous reduction of diazonium salts. Appl. Surf. Sci. 314 (2014) 358-366.

[28] P. Allongue, C.H. De Villeneuve, J. Pinson, F. Ozanam, J.N. Chazalviel, X. Wallart, Organic monolayers on Si (111) by electrochemical method. Electrochim. Acta. 43 (1998) 2791-2798.

[29] P. Allongue, C.H. de Villeneuve, J. Pinson, Structural characterization of organic monolayers on Si <111> from capacitance measurements. Electrochim. Acta. 45 (2000) 3241-3248.

[30] R. Haight, L. Sekaric, A. Afzali, D. Newns, Controlling the electronic properties of silicon nanowires with functional molecular groups. Nano Lett. 9 (2009) 3165-3170.

[31] K. Balasubramanian, M. Burghard, Chemically functionalized carbon nanotubes. Small 1 (2005) 180-192.

[32] L. Fan, J. Chen, S. Zhu, M. Wang, G. Xu, Determination of Cd2+ and Pb2+ on glassy carbon electrode modified by electrochemical reduction of aromatic diazonium salts. Electrochem. Commun. 11 (2009) 1823-1825.

[33] A. Roglans, A. Pla-Quintana, M. Moreno-Manas, Diazonium salts as substrates in palladium-catalyzed cross-coupling reactions. Chem. Rev. 106 (2006) 4622-4643.

[34] C. Bourdillon, M. Delamar, C. Demaille, R. Hitmi, J. Moiroux, J. Pinson, Immobilization of glucose oxidase on a carbon surface derivatized by electrochemical reduction of diazonium salts. J. Electroanal. Chem. 336 (1992) 113-123.

[35] CasaXPS software, http://www.casaxps.com/

[36] B. Chen, A.K. Flatt, H. Jian, J.L. Hudson, J.M. Tour, Molecular grafting to silicon surfaces in air using organic triazenes as stable diazonium sources and HF as a constant hydride-passivation source. Chemistry of materials, 17 (2005) 4832-4836.

[37] G. Liu, T. Böcking, J.J. Gooding, Diazonium salts: Stable monolayers on gold electrodes for sensing applications. J. Electroanal. Chem. 600 (2007) 335-344.

[38] M. Liu, R Liu, W. Chen, Graphene wrapped Cu2O nanocubes: non-enzymatic electrochemical sensors for the detection of glucose and hydrogen peroxide with enhanced stability. Biosens. Bioelectron. 45 (2013) 206-212.

[39] R. Nasraoui, D. Floner, F. Geneste, Improvement in performance of a flow electrochemical sensor by using carbamoyl-arms polyazamacrocycle for the preconcentration of lead ions onto the electrode. Electrochem. Commun. 12 (2010) 98-100.